Whole-Volume Tumor MRI Radiomics for Prognostic Modeling in Endometrial Cancer

Kristine E. Fasmer, MSc,[1,2*] Erlend Hodneland, PhD,[1,3] Julie A. Dybvik, MD,[1,2] Kari Wagner-Larsen, MD,[1,2] Jone Trovik, MD PhD,[4,5] Øyvind Salvesen, PhD,[6] Camilla Krakstad, PhD,[4,5] and Ingfrid H.S. Haldorsen, MD PhD[1,2*]

Background: In endometrial cancer (EC), preoperative pelvic MRI is recommended for local staging, while final tumor stage and grade are established by surgery and pathology. MRI-based radiomic tumor profiling may aid in preoperative risk-stratification and support clinical treatment decisions in EC.
Purpose: To develop MRI-based whole-volume tumor radiomic signatures for prediction of aggressive EC disease.
Study Type: Retrospective.
Population: A total of 138 women with histologically confirmed EC, divided into training (n_T = 108) and validation cohorts (n_V = 30).
Field Strength/Sequence: Axial oblique T_1-weighted gradient echo volumetric interpolated breath-hold examination (VIBE) at 1.5T (71/138 patients) and DIXON VIBE at 3T (67/138 patients) at 2 minutes postcontrast injection.
Assessment: Primary tumors were manually segmented by two radiologists with 4 and 8 years' of experience. Radiomic tumor features were computed and used for prediction of surgicopathologically-verified deep (≥50%) myometrial invasion (DMI), lymph node metastases (LNM), advanced stage (FIGO III + IV), nonendometrioid (NE) histology, and high-grade endometrioid tumors (E3). Corresponding analyses were also conducted using radiomics extracted from the axial oblique image slice depicting the largest tumor area.
Statistical Tests: Logistic least absolute shrinkage and selection operator (LASSO) was applied for radiomic modeling in the training cohort. The diagnostic performances of the radiomic signatures were evaluated by area under the receiver operating characteristic curve in the training (AUC_T) and validation (AUC_V) cohorts. Progression-free survival was assessed using the Kaplan–Meier and Cox proportional hazard model.
Results: The whole-tumor radiomic signatures yielded AUC_T/AUC_V of 0.84/0.76 for predicting DMI, 0.73/0.72 for LNM, 0.71/0.68 for FIGO III + IV, 0.68/0.74 for NE histology, and 0.79/0.63 for high-grade (E3) tumor. Single-slice radiomics yielded comparable AUC_T but significantly lower AUC_V for LNM and FIGO III + IV (both $P < 0.05$). Tumor volume yielded comparable AUC_T to the whole-tumor radiomic signatures for prediction of DMI, LNM, FIGO III + IV, and NE, but significantly lower AUC_T for E3 tumors ($P < 0.05$). All of the whole-tumor radiomic signatures significantly predicted poor progression-free survival with hazard ratios of 4.6–9.8 ($P < 0.05$ for all).
Data Conclusion: MRI-based whole-tumor radiomic signatures yield medium-to-high diagnostic performance for predicting aggressive EC disease. The signatures may aid in preoperative risk assessment and hence guide personalized treatment strategies in EC.
Level of Evidence: 4
Technical Efficacy Stage: 2

J. MAGN. RESON. IMAGING 2021;53:928–937.

View this article online at wileyonlinelibrary.com. DOI: 10.1002/jmri.27444

Received Sep 1, 2020, Accepted for publication Oct 30, 2020.

*Address reprint requests to: Kristine E. Fasmer, Mohn Medical Imaging and Visualization Centre, Haukeland University Hospital, Jonas Lies vei 65, Postbox 7800, 5021 Bergen, Norway. E-mail: kristine.fasmer@helse-bergen.no; Ingfrid H.S. Haldorsen, Mohn Medical Imaging and Visualization Centre, Haukeland University Hospital, Jonas Lies vei 65, Postbox 7800, 5021 Bergen, Norway. E-mail: ingfrid.haldorsen@helse-bergen.no
Contract grant sponsor: Western Norway Regional Health Authority; Contract grant number: 912060; Contract grant sponsor: University of Bergen, and Bergen Research Foundation; Contract grant number: BFS2019TMT06.

From the [1]Department of Radiology, Mohn Medical Imaging and Visualization Centre (MMIV), Haukeland University Hospital, Bergen, Norway; [2]Section for Radiology, Department of Clinical Medicine, University of Bergen, Bergen, Norway; [3]NORCE Norwegian Research Centre, Bergen, Norway; [4]Department of Obstetrics and Gynaecology, Haukeland University Hospital, Bergen, Norway; [5]Centre for Cancer Biomarkers, Department of Clinical Science, University of Bergen, Bergen, Norway; and [6]Unit for applied Clinical Research, Department of Public Health and Nursing, Norwegian University of Science and Technology, Trondheim, Norway

Additional supporting information may be found in the online version of this article

PRECISION MEDICINE is an evolving field in cancer research that attempts to capitalize on the vast amounts of patient-specific data derived from, eg, histological or imaging-based tumor profiling, in order to develop more individualized treatment strategies that optimize the therapeutic benefit. Endometrial cancer (EC) is the most common gynecological cancer in industrialized countries and the incidence rate has been steadily increasing over the past decades.[1] With a 5-year survival rate of 84%, the overall prognosis of EC is good.[2] However, a clinical dilemma faced in EC is overtreatment in low-risk patients, leading to unnecessary side effects. Oxymoronically, another problem is undertreatment in undetected high-risk patients in whom a more aggressive treatment strategy would improve survival.[3] Thus, EC patients would potentially benefit from refined tools with which to guide precision medicine approaches as opposed to one-size-fits-all treatment strategies.

ECs are surgicopathologically staged according to the International Federation of Gynecology and Obstetrics (FIGO 2009) system, which incorporates information on local tumor extent and metastatic spread.[4,5] However, contrast-enhanced (CE) pelvic magnetic resonance imaging (MRI), being the imaging method of choice for preoperative local staging, is widely performed and guides the choice of primary surgical treatment.[6,7] In addition to standard MRI findings suggesting advanced stage (ie, deep myometrial invasion, cervical stroma invasion, and enlarged pelvic lymph nodes), large tumor volume and large maximum tumor diameter at MRI have also been shown to predict poor prognosis in EC.[8–10]

Radiomic tumor profiling involves the extraction of large amounts of quantitative imaging features that can be utilized in multiparametric models for disease characterization and prediction of clinical and biological outcomes.[11–13] Specific radiomic tumor profiles predict the stage and clinical phenotype in various cancers, thus presenting a promising approach to enable accurate staging, prognostication, and more tailored treatment strategies.[14–18] A few recent studies have also explored MRI-based radiomic tumor features in EC and linked these to an aggressive phenotype.[19–23] However, some of these studies[19,20] are based on single-slice radiomic profiling. As single-slice images only cover a proportionally small part of the tumor, they may not necessarily be representative of the entire tumor.

The purpose of the present study was to conduct MRI-based whole-volume radiomic tumor profiling in a population-based cohort of EC patients and link specific whole-tumor radiomic signatures to surgicopathological markers of aggressive EC disease. Furthermore, we aimed to compare the diagnostic performance of whole-tumor radiomic signatures with that of single-slice radiomic signatures for predicting high-risk disease in the same EC patient cohort.

Materials and Methods

Patients, Treatment, and Surgicopathological Staging

This retrospective study included 138 women with histologically confirmed endometrial carcinoma who all underwent pelvic MRI prior to surgicopathological staging between 2009 and 2019. The patients were randomly selected from a larger prospective population-based study cohort in Hordaland County (Norway), which was conducted under Institutional Review Board (IRB)-approved protocols (IRB approvals: 2015/2333; 2015/548; biobank approval 2015/1907) with written informed consent from all patients. Since 2009, preoperative pelvic MRI has been included as a part of this prospective study, using standardized imaging protocols (Table 2). From preoperative biopsy the patients were graded as either low-risk (endometrioid grade 1–2 [E1-E2]) or high-risk (endometrioid grade 3 [E3] or nonendometrioid [NE]) EC.

All of the 138 patients in the cohort underwent hysterectomy with bilateral salpingo-oophorectomy; 52% (72/138) had pelvic lymph node sampling, while 17% (23/138) had accompanying paraaortic lymph node sampling. Surgical specimens were assessed by pathologists using standard procedures[24] and the presence of deep (≥50%) myometrial invasion (DMI), lymph node metastases (LNM), and tumor histologic subtyping and grading (E1, E2, E3, or NE) were confirmed microscopically. The patients were surgically staged according to the FIGO 2009 criteria.[4,5] Adjuvant treatment were given to 33% (46/138) of the patients, chemotherapy to 30% (42/138), external radiation therapy to 2% (3/138), and brachytherapy to 1% (1/138) of the patients.

Patient and surgicopathological characteristics for the 138 EC patients are given in Table 1. The mean (range) time span between the MRI examination and surgical staging was 16 (1–84) days and all patients were diagnosed and treated at the same university hospital. Patient follow-up data were collected from patient medical records and from correspondence with the responsible physicians/gynecologists, as previously described.[25] Mean (range) follow-up time was 40 (0, 102) months and date of last follow-up was November 21st, 2019. Progression was defined as local recurrence/progression in the pelvis or new metastases in the abdomen or at distant sites.

These patients were divided into a training cohort of 108 patients for radiomic feature selection and prediction model generation, with the remaining 30 patients in a validation cohort for testing of the proposed radiomic signatures. This division was conducted in a supervised manner to assure similar frequencies for the surgicopathological outcomes in the training and validation cohorts (Table S1).

MRI Scanning

Preoperative pelvic MRI was acquired with a 1.5T Avanto scanner for 71/138 patients and with a 3T Skyra scanner for the remaining 67/138 (Siemens, Erlangen, Germany). Patient and surgicopathological characteristics for patients according to scanner/protocol are given in Table S2. To reduce bowel peristalsis, 20 mg butylscopoalmine bromide (Buscopan, Boehringer Ingelheim, Germany) was administered intramuscularly/intravenously to all patients prior to imaging. The MRI protocols included sagittal and axial

TABLE 1. Characteristics for the Endometrial Cancer Patients (*n* = 138)

Age, median (range)	67 (39–90)
BMI, median (range)	26 (16–53)
Postmenopausal, *n* (%), *n* = 137	125 (91%)
Risk status[a] from preoperative biopsy/curettage, *n* (%)	
Low-risk	91 (66%)
High-risk	35 (25%)
Missing	12 (9%)
Myometrial invasion, *n* (%)	
< 50%	77 (56%)
≥ 50%	61 (44%)
Lymphadenectomy, *n* (%)	
Pelvic	72 (52%)
Pelvic+para-aortic	23 17%)
No	43 (31%)
Lymph node metastases, *n* (%)	
Pelvic only	11 (8%)
Para-aortic +/− pelvic	3 (2%)
Confirmed negative	81 (59%)
Not investigated	43 (31%)
FIGO stage, *n* (%)	
I	109 (79%)
II	10 (7)
III	17 (12%)
IV	2 (2%)
Histologic subtype, *n* (%)	
Endometrioid	113 (82%)
Clear cell	6 (4%)
Serous papillary	11 (8%)
Carcinosarcoma	5 (4%)
Undifferentiated/other	3 (2%)
Histologic grade, *n* (%)	
E1	54 (39%)
E2	34 (25%)
E3	22 (16%)
NE	23 (17%)
Missing	5 (4%)

BMI: body mass index; FIGO: the International Federation Of Gynecology And Obstetrics system; E1: endometrioid grade 1; E2: endometrioid grade 2; E3: endometrioid grade 3; NE: nonendometrioid.
[a]Risk status based on preoperative biopsy (low-risk: E1 + E2; high-risk: E3 + NE).

oblique T_2-weighted turbo spin echo imaging, axial oblique T_1-weighted gradient echo volumetric interpolated breath-hold examination (VIBE) (1.5T), and VIBE DIXON (3T) imaging before and 2 minutes after administration of contrast agent (0.1 mmol gadolinium/kg body weight, Dotarem, Guerbet, France) and axial oblique diffusion-weighted imaging (DWI) with b-values of 0 and 1000 s/mm^2 (1.5T) or 0. 500 and 1000 s/mm^2 (3T). Protocols at both field strengths (Table 2) are in line with the recommended guidelines of the European Society of Urogenital Imaging.[26]

Tumor Segmentation and Radiomic Feature Extraction

For the purpose of tumor segmentation, the T_1-weighted axial oblique images acquired at 2 minutes postcontrast injection were used, since this sequence and contrast delay provides the best discrimination between tumor tissue and normal surrounding myometrial tissue.[6,27] The endometrial primary tumors were manually delineated using the free, open-source software application ITK-SNAP (www.itksnap.org, v. 3.6.0) (Fig. 1). The segmentations were conducted by one of two radiologists, (J.A.D. and K.W.L., having 4 and 8 years' experience, respectively, in pelvic MRI reading) who were blinded to clinical and pathological patient information. Although not used for segmentation, the DWI and T_2-weighted series were available to the readers for visual inspection to verify tumor borders.

In total, 15 radiomic tumor features were extracted from the tumor masks: tumor volume, tumor volume-to-surface ratio (surfvolratio), gray-level (GL) histogram features (kurtosis, skewness, entropy), GL cluster features (cluster-size and -index), gray-level co-occurrence matrix (GLCM) features (energy, homogeneity, contrast, correlation), and gray-level run length matrix (GLRLM) features (short- and long-run emphasis [SRE, LRE] and low- and high gray-level run emphasis [LGRE, HGRE]) (Fig. 1). The radiomic features were computed by algorithms implemented in Python (www.python.org), following the IBSI standards,[28] and normalized for each scanner/protocol using standard z-scores.

In order to investigate the stability of the derived radiomic features when extracted from tumor masks delineated by different readers, 35 randomly chosen patients were selected for tumor segmentation by both readers. For comparison of whole-tumor radiomic profiling with single-slice radiomic profiling, the axial oblique image planes depicting the largest tumor mask area were identified and all the radiomics features were also extracted from these single-slice masks.

TABLE 2. MRI Scanning Protocols

MR scanner	Sequence	Dim	Plane	TR/TE_1/TE_2 (ms)	FA (deg)	Slice/Incr (mm)	Matrix	FOV (mm)	Pixel (mm)
1.5T Siemens Avanto	T_2 TSE	2D	AO	6310/95	150	3.0/3.3	256 × 256	180 × 180	0.9 × 0.7
	T_2 TSE	2D	SAG	4920/95	150	3.0/3.3	256 × 256	180 × 180	0.9 × 0.7
	DWI	2D	AO	3100/79	90	5.0/6.0	128 × 128	300 × 300	2.3 × 2.3
	T_1 VIBE	3D	AO	7.2/2.6	20	2.0/2.0	192 × 154	250 × 250	1.6 × 1.3
3T Siemens Skyra	T_2 TSE	2D	AO	4330/94	150	3.0/3.3	326 × 384	200 × 200	0.5 × 0.5
	T_2 TSE	2D	SAG	7360/101	160	3.0/3.3	310 × 320	200 × 200	0.6 × 0.6
	DWI RESOLVE	2D	AO	6010/74/126	180	3.0/3.3	144 × 144	200 × 200	1.4 × 1.4
	T_1 DIXON	3D	AO	5.9/2.5/3.7	9	1.2/1.2	139 × 256	250 × 250	1.0 × 1.0

AO: axial oblique slice orientation; Deg: degrees; Dim: dimension; DWI: diffusion weighted imaging; FA: flip angle; FOV: field of view; Incr: increment between slices; RESOLVE: Readout Segmentation Of Long Variable Echo trains; TE: time echo; TR: repetition time; TSE: turbo spin echo; VIBE: volumetric interpolated breath-hold examination.

Statistical Analyses

The stability of the radiomic features extracted from different tumor masks (delineated by the two readers) and different scanners (Table 2) were assessed by intraclass correlation coefficients (ICCs) and Mann–Whitney *U*-tests, respectively. The radiomic features having ICC > 0.75 between readers/segmentations and with $P > 0.05$ in the Mann–Whitney *U*-test between scanners were considered stable and retained for further analyses (Table S3). This resulted in a whole-tumor radiomic dataset consisting of 14 features (kurtosis excluded) and a single-slice dataset consisting of 12 features (surfvolratio, cluster-size, and entropy excluded).

Logistic radiomic models for prediction of surgicopathological outcomes were derived in the training cohort by the use of least absolute shrinkage and selection operator (LASSO) and Elastic net (Enet) regression (Fig. 1). The penalty parameters (λ and α) were selected by 10-fold cross-validation and minimization of the cross-validation function. For a complete list of the whole-tumor radiomic features selected by LASSO and Enet regression, please refer to Table S4. The derived radiomic signatures were evaluated in both the training and validation sets by deviance from goodness-of-fit analyses ($deviance_T$, $deviance_V$), and by area under the receiver operating characteristic (ROC) curves (AUC_T and AUC_V in the training and validation cohorts, respectively). All analyses were conducted using both the whole-tumor- and single-slice-derived radiomic features, separately. The resulting AUCs were compared using DeLong's test of equality.

For the LASSO radiomic signatures derived in the training cohort, optimal cutoffs were identified from the ROC curves using the Youden Index. The prognostic value of the categorized radiomic signatures was explored using the Kaplan–Meier estimator with log-rank test and the Cox proportional hazard model for prediction of progression-free survival.

All statistical analyses were performed with STATA 16.1 (StataCorp, College Station, TX), and the reported *P* values were generated by two-sided tests and considered significant when less than 0.05.

Results

Enet, which linearly combines LASSO and ridge regression, selected more of the features compared to LASSO alone, but this did not improve the goodness of fit ($deviance_{T,V}$, Table S4) nor the areas under the predicted ROC curves ($AUC_{T,V}$) (Table S5). Hence, the LASSO model was used for further analyses.

Whole Tumor vs. Single-Slice Radiomic LASSO Signature Modeling

The whole-tumor LASSO radiomic signatures yielded AUC_T/AUC_V of 0.84/0.76 for predicting DMI, 0.73/0.72 for LNM, 0.71/0.68 for FIGO III + IV, 0.68/0.74 for NE histology, and 0.79/0.63 for high grade (Table 3). Corresponding metrics for single-slice-derived LASSO radiomic signatures (Table S6) were AUC_T/AUC_V of 0.85/0.77 for DMI, 0.83/0.56 for LNM, 0.72/0.56 for FIGO III + IV, 0.68/0.73 for NE histology, and 0.75/0.63 for high grade. In the training cohort no significant differences in the AUC_T for the whole-tumor and single-slice signatures were observed, whereas in the validation cohort the whole-tumor signature yielded significantly higher AUC_V than the single-slice signature for prediction of LNM (0.72 vs. 0.56; $P < 0.05$) and tended to the same for advanced FIGO stage (0.68 vs. 0.56; $P = 0.05$) (Table 3).

Whole-Tumor Radiomic LASSO Signature vs. Biopsy Risk Status and MRI Tumor Volume

The derived whole-tumor radiomic signatures had significantly higher AUC_T compared to preoperative biopsy assessed

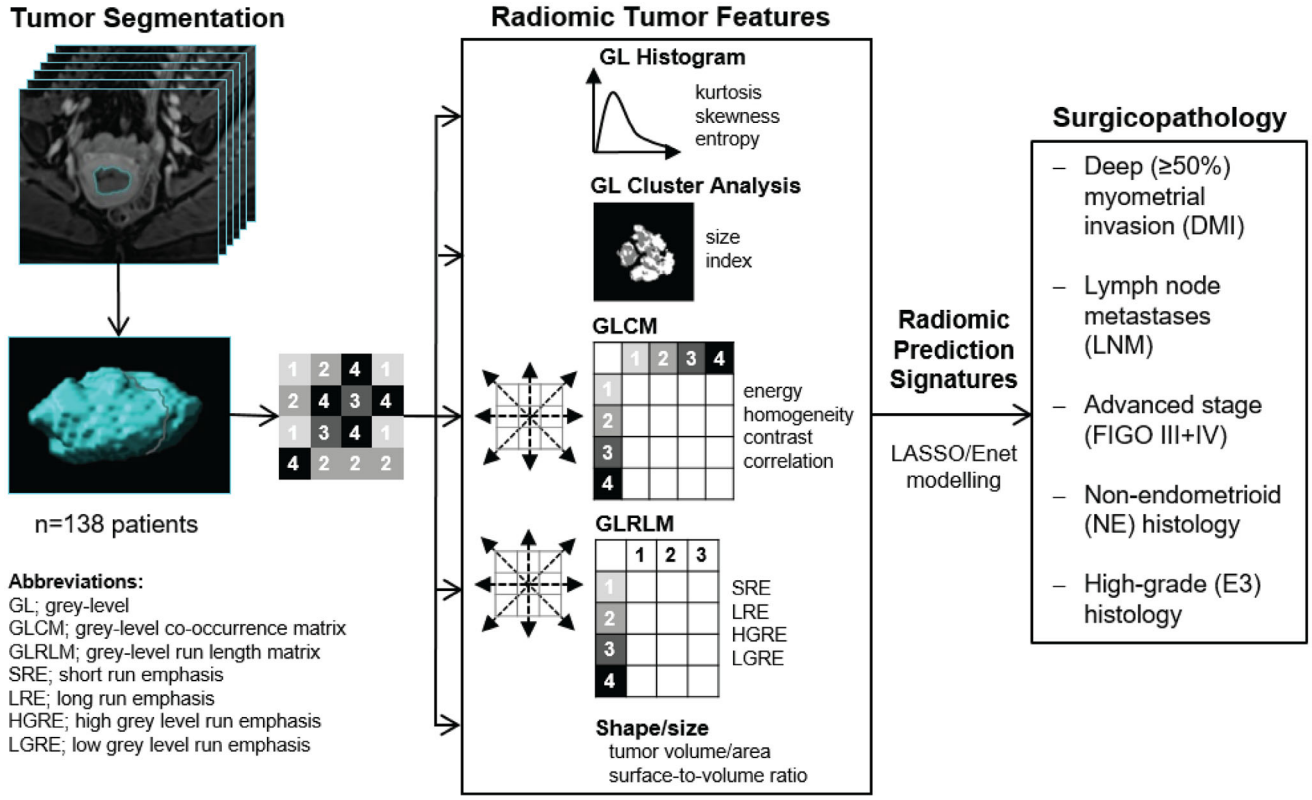

FIGURE 1: Outline of the project workflow consisting of whole-volume (whole-tumor) manual tumor segmentation on axial oblique contrast-enhanced T_1-weighed images, radiomic tumor feature extraction, and construction of radiomic signatures for prediction of high-risk surgicopathological features in 138 EC patients. Radiomic signatures were derived based on the whole-tumor masks (whole-tumor radiomics) and separately based on single-slice masks (single-slice radiomics) using only the single image slice depicting the largest tumor area. Least absolute shrinkage and selection operator (LASSO) and elastic net (Enet) were applied for prediction modeling.

high-risk (E3 + NE) histology for prediction of surgicopathological DMI (AUC_T: 0.84 vs. 0.55, $P < 0.05$) and LNM (AUC_T: 0.73 vs. 0.58, $P < 0.05$), while significantly lower AUC_T for prediction of NE histology (AUC_T: 0.68 vs. 0.90, $P < 0.05$). For prediction of advanced FIGO stage and high-grade tumor, AUCs for whole-tumor signatures and preoperative high-risk histology were similar (P = 0.61 and 0.99, respectively) (Fig. 2). When comparing the whole-tumor radiomic signatures with tumor volume as an individual predictor, only the signature for prediction of high-grade tumor yielded significantly higher AUC_T (AUC_T: 0.79 vs. 0.68, $P < 0.05$), whereas the AUCs for prediction of DMI, LNM, FIGO III + IV, and NE histology were similar (P = 0.39, 0.80, 1.00 and 0.71, respectively) (Fig. 2).

Whole-Tumor Radiomic LASSO Signature for Prediction of Progression-Free Survival

Based on the whole-tumor radiomic signature ROC curves in the training cohort (Fig. 2), we established the optimal cutoffs for prediction of each outcome (DMI, LNM, advanced FIGO stage, NE histology, and high-grade tumor) and dichotomized the whole-tumor signatures for the complete cohort (n = 138) accordingly. The dichotomized whole-tumor radiomic signatures were all significantly associated with reduced survival ($P < 0.05$ for all, Fig. 3), both in univariate analyses with hazard ratios (HRs) in the range of 4.6–9.8 ($P < 0.05$ for all, Table 4) and after adjusting for high-risk histology in preoperative biopsy (HR: 3.2–8.0, $P < 0.05$ for all, Table 4).

Discussion

This study supports the promising role of whole-tumor radiomic tumor profiling for accurate preoperative staging and prognostication in EC. The derived MRI-based whole-tumor radiomic tumor signatures yielded medium-to-high diagnostic performance metrics for prediction of high-risk surgicopathological features and poor outcome in EC. When comparing the diagnostic performance of single-slice- vs. whole-tumor-derived radiomic signatures, single-slice and whole-tumor signatures yielded similar performance metrics in the training cohort, but interestingly, the whole-tumor signatures outperformed single-slice signatures for prediction of LNM and advanced FIGO stage in the validation cohort. These findings suggest a possible advantage of whole-tumor over single-slice radiomic profiling in EC, incorporating information from the entire tumor and not only from a central part of the tumor. Importantly, the radiomic signatures

TABLE 3. Receiver Operating Characteristics (ROC) Analyses for Prediction of Deep (≥50%) Myometrial Invasion (DMI), Lymph Node Metastases (LNM), FIGO Stage III + IV, Nonendometrioid (NE) Histology, and High Grade (E3) based on LASSO Radiomic Single-Slice and Whole-Tumor Volume Signatures

	Predicted ROC training				Predicted ROC validation			
Radiomic signatures	**n_T[a]**	**tumor AUC_T**	**slice AUC_T**	***P*[b]**	**n_V[a]**	**tumor AUC_V**	**slice AUC_V**	***P*[b]**
DMI	51/108	0.84	0.85	0.71	10/30	0.76	0.77	0.72
LNM	11/74[c]	0.73	0.83	0.16	3/21[c]	0.72	0.56	*0.01*
FIGO III + IV	15/108	0.71	0.72	0.75	4/30	0.68	0.56	0.05
NE histology	21/108	0.68	0.68	0.91	4/30	0.74	0.73	0.87
High grade (E3)	16/86[d]	0.79	0.75	0.28	5/24[d]	0.63	0.63	1.00

Area under the curves (AUC) are given for both the training (AUC_T) and the validation (AUC_T) cohorts.
LASSO: least absolute shrinkage and selection operator; FIGO: the International Federation Of Gynecology And Obstetrics system; NE: nonendometrioid; E3: endometrioid grade 3.
[a]Number of patients with outcome of interest/total number of patients in cohort.
[b]*P* values refer to DeLong test of equality of ROC areas. Significant *P* values are given in italics.
[c]Number of patients with lymphadenectomy.
[d]Number of patients with endometrioid subtype.

also yielded comparable (for predicting DMI, LNM, advanced FIGO stage, and NE histology) or slightly better (for high-grade histology) diagnostic performance to that of MRI-based tumor volume (analyzed individually), confirming the well-known role of tumor volume as a predictor of high-risk surgicopathological features and poor outcome in EC.[8–10,29,30]

Only a few studies, to our knowledge, have explored MRI radiomics in EC. Ueno et al[19] and Ytre-Hauge et al[20] (n = 137 and n = 180 EC patients, respectively) both reported that radiomic features extracted from primary tumor segmentations in a single image plane (single-slice radiomics) were associated with markers of aggressive disease (ie, DMI and high-risk histology). Ytre-Hauge et al,[20] however, did not report on radiomic modeling and neither Ueno et al[19] nor Ytre-Hauge et al[20] validated their findings in a separate validation cohort. In a recent study of 54 EC patients, using full tumor segmentations on T_2-weighted images, Stanzione et al found that their random forest-based radiomic model was able to predict DMI with an AUC of 0.92 and 0.94 in the training and validation/test sets, respectively.[23] In our larger study cohort (n = 138), with tumor segmentations on CE T_1-weighted images that reportedly discriminates better between EC tissue and the surrounding normal myometrium,[6,27] we, however, found a somewhat lower AUC for predicting DMI, both in the training and the validation sets (AUC_T = 0.84, AUC_V = 0.74). Given the differences between the two studies, both with respect to cohort sizes (54 vs. 108 patients), imaging sequence (T_2 vs. CE T_1), and statistical method (random forest vs. LASSO/Enet), it is difficult to draw any firm conclusions regarding the reason for the observed difference in diagnostic performance of the radiomic models. Importantly, both models would need to be validated in independent EC cohorts prior to potential implementation in the clinic. For preoperative prediction of LNM in EC, Xu et al recently explored several prediction models incorporating MRI radiomics.[21] The model based on multiplanar whole-tumor CE MRI radiomics alone yielded AUCs of 0.79/0.75 (training cohort (n = 140) / test cohort (n = 60)), which is somewhat higher compared to our performance metrics for prediction of LNM (AUC_T = 0.73, AUC_V = 0.72). The prevalence of LNM, however, is substantially higher in the study by Xu et al (37% and 25% in the training and test cohorts, respectively) compared to our study (15% and 14% in the training and validation cohorts, respectively), which may have influenced the prediction models and hence makes direct comparisons of the performance metrics difficult. The prevalence of LNM in our study is, nonetheless, representative of that reported in other population-based cohorts[31] and the diagnostic performance metrics of the radiomic models presented here are thus likely to be transferable to other population-based EC patient cohorts. Xu et al also found that a model incorporating both radiomic features and clinical parameters (CA 125 and MRI-assessed LN size) yielded higher AUCs of 0.89/0.88 for predicting LNM than the model incorporating radiomics alone.[21] Since the scope of our study went beyond predicting LNM (by also including DMI, advanced FIGO stage, NE histology, and high tumor grade), we chose not to incorporate other clinical (preoperative) parameters (such as MRI-assessed LN size) in the present study.

Deriving whole-tumor radiomics signatures is a time-consuming process, since it requires manual delineation of the tumor borders on several image slices by highly

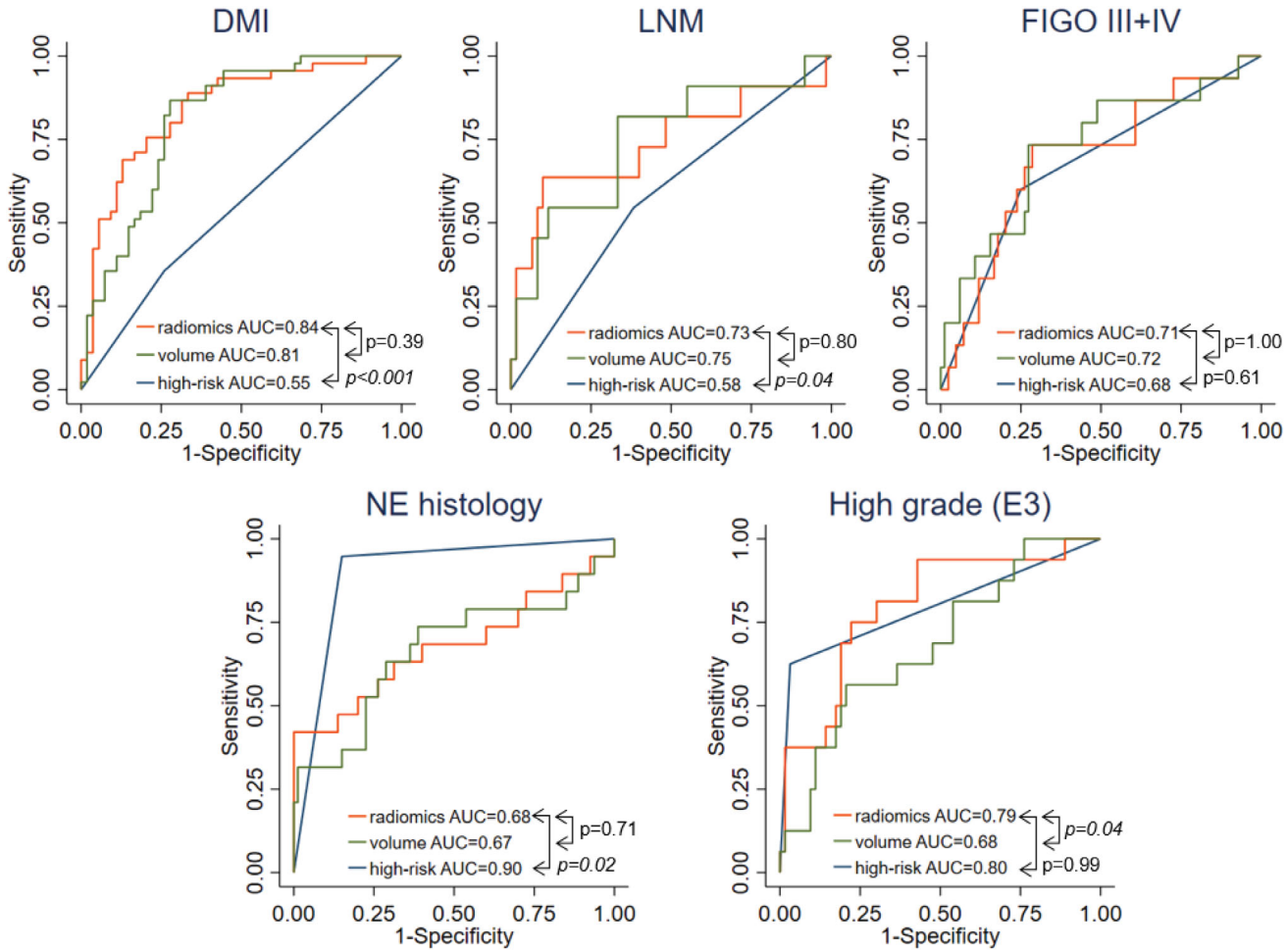

FIGURE 2: Receiver operating characteristic (ROC) curves in the training cohort (n_T = 108) for prediction of deep (≥50%) myometrial invasion (DMI), lymph node metastases (LNM), FIGO stage III + IV, nonendometrioid (NE) histology, and high-grade tumor (E3), based on the whole-tumor LASSO radiomic signatures, tumor mask volume, and preoperative high-risk histology (from biopsy). Equality of areas under the ROC curves (AUCs) were assessed by the DeLong test, with significant *P* values given in italics.

specialized radiologists. Although the findings in this study suggest that whole-tumor radiomics may prove superior to single-slice radiomics for capturing the radiomic markers relevant for clinical phenotyping in EC, they need to be validated in independent and larger EC cohorts before any firm conclusions can be drawn. Fortunately, machine-/deep-learning-based imaging tools that will allow automated whole-volume tumor segmentations are likely to be developed in the near future, reducing the time-consuming manual steps presently needed to generate whole-tumor radiomic profiles.

The whole-tumor prediction models in this study were all developed using datasets consisting of both radiomic features (GL histogram, GL clusters, GLCM, GLRLM) and MRI-based tumor size (whole-tumor volume / single-slice tumor area). Tumor volume/area was selected by LASSO (and Enet) for all of the surgicopathological outcomes except DMI, and hence was incorporated in the resulting radiomics signatures. Interestingly, when comparing the whole-tumor radiomic signatures to tumor volume alone, we found no significant differences in their diagnostic performance metrics except for prediction of high-grade tumors (E3), for which the whole-tumor radiomic signature yielded significantly higher AUC_T than that of tumor volume alone. These findings reaffirm the well-established predictive- and prognostic role of tumor size/volume in EC, with a vast literature consistently linking large tumor size to advanced stage and poor survival.[8–10,29,30]

Limitations

First, several of the high-risk surgicopathological features that we aimed to predict preoperatively by using MRI radiomics were relatively rare. Particularly, information on surgicopathological LNM status, which is a strong prognostic factor in EC, will in most population-based cohorts be incomplete, due to international guidelines recommending lymphadenectomy/lymph node dissection only in high-to-intermediate risk patients.[32] This is challenging, both when building the prediction modeling in the test cohort and for validation in the smaller validation cohort. Second, we did not include all of the available image sequences in the radiomics analyses, resulting in a relatively small number

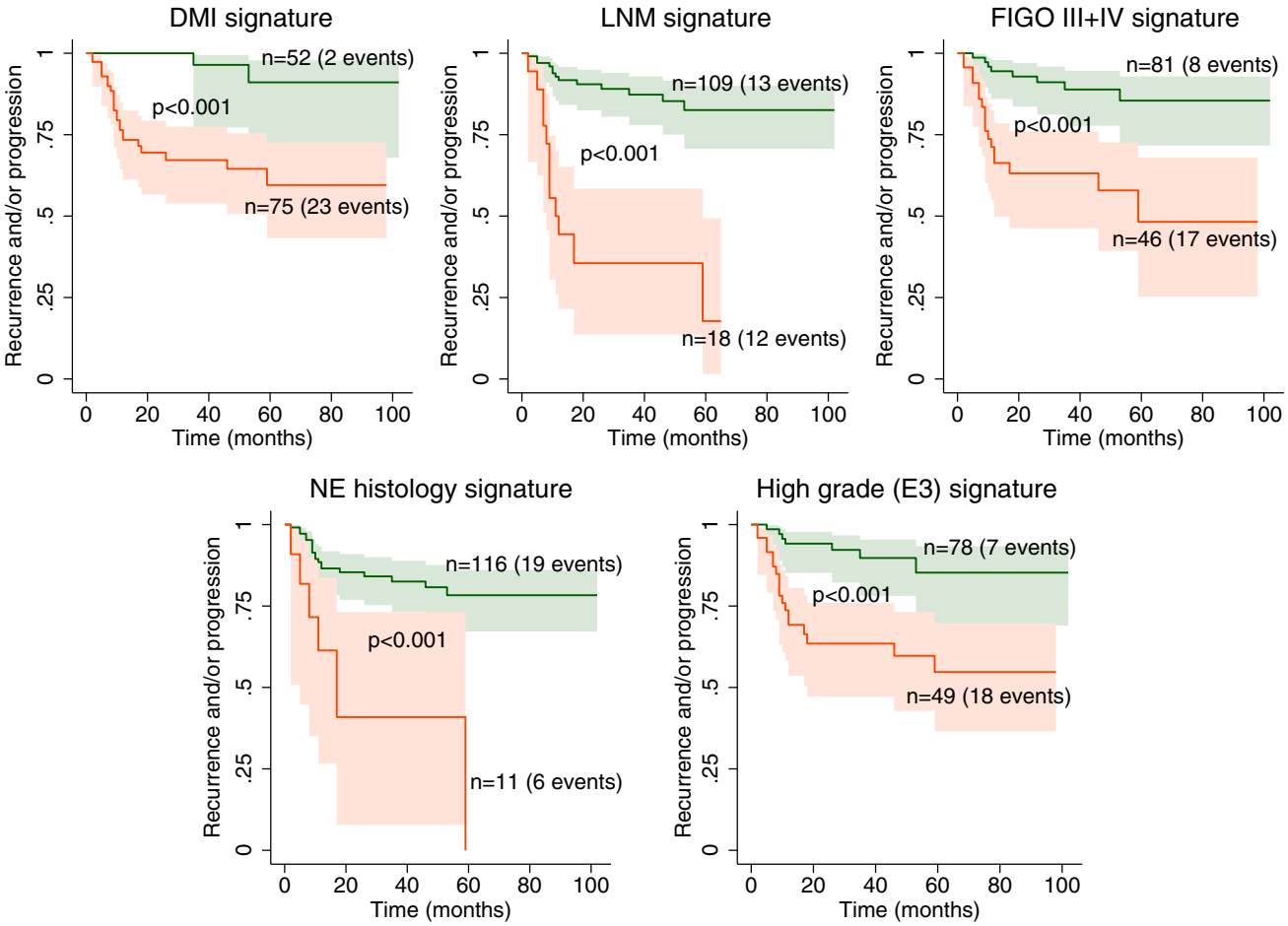

FIGURE 3: Kaplan–Meier survival curves depicting progression-free survival in the endometrial cancer cohort (*n* = 138), using the LASSO whole-tumor signatures derived in the training set (n_T = 108) for prediction of deep (≥50%) myometrial invasion (DMI), lymph node metastases (LNM), FIGO stage III + IV, nonendometrioid (NE) histology, and high-grade tumor (E3). The green and red curves represent patients with whole-tumor radiomic signatures above and below each signature's cutoff, respectively. The cutoffs are identified from receiver operating characteristics curves in the training cohort using the Youden Index.

TABLE 4. Cox Regression Analyses for Prediction of Progression-Free Survival in Endometrial Cancer (*n* = 138 Patients), Using the LASSO Whole Tumor Radiomic Signatures for Prediction of Deep (≥50%) Myometrial Invasion (DMI), Lymph Node Metastases (LNM), FIGO stage III + IV, Nonendometrioid (NE) Histology, and High Grade (E3)

Whole tumor radiomic signature cutoff	Univariate HR (95% CI)	P[a]	Adjusted[b] HR (95% CI)	P[a]
DMI	9.8 (2.3–41.7)	*0.002*	8.0 (1.9–34.3)	*0.005*
LNM	7.7 (3.5–17.2)	*<0.001*	5.5 (2.3–13.0)	*<0.001*
FIGO III + IV	4.9 (2.1–11.4)	*<0.001*	3.8 (1.6–9.1)	*0.003*
NE histology	5.0 (2.0–12.8)	*0.001*	3.2 (1.1–9.1)	*0.03*
High grade (E3)	4.6 (1.9–11.0)	*<0.001*	3.7 (1.5–9.0)	*0.004*

The signatures are dichotomized with cutoffs based on the Youden Index (YI) for the ROC curves in the training cohort for each of the surgicopathological outcomes.
HR: hazard ratio; CI: confidence interval; DMI: deep myometrial invasion; LNM: lymph node metastases; LASSO: least absolute shrinkage and selection operator; FIGO: the International Federation Of Gynecology And Obstetrics system; NE: nonendometrioid; E3: endometrioid grade 3; YI: Youden Index.
[a]Significant *P* values are given in italics.
[b]Adjusted for high-risk histology (endometrioid grade 3 or nonendometrioid histology) based on preoperative biopsy.

of radiomics features extracted (15 in total). We might, thereby, have missed radiomic features from other MRI sequences that potentially could have improved the predictive power of the radiomic signatures. Automated tumor mask registrations across series were, however, not feasible due to large organ movement during scanning. Manual segmentation of the tumors on all the different image series are possible, but were regarded as too time-consuming for the radiologists involved in the project. Finally, the use of two different protocols/scanners might have influenced image quality, and hence tumor segmentation accuracy and radiomic feature extraction. Nevertheless, the included CE T_1-based radiomic features exhibited a high level of stability (with only a few features excluded from the analyses), both across scanners and across observers/segmentations, which we consider a strength of the study.

Conclusion

The developed MRI-based whole-tumor radiomic signatures yielded medium-to-high AUCs for prediction of DMI, LNM, and advanced FIGO stage, both in the training and validation sets and predicted poor outcome. However, the whole-tumor radiomic signatures did not outperform tumor volume (analyzed individually) except for the prediction of high-grade histology. Whole-tumor- and single-slice-derived radiomic signatures yielded similar AUCs for predicting aggressive EC disease in the training cohort, whereas the whole-tumor radiomics signatures outperformed single-slice signatures in the validation cohort. This study supports the promising role of whole-tumor radiomic tumor profiling for refined preoperative clinical phenotyping guiding personalized treatment strategies in EC.

REFERENCES

1. Bray F, Ferlay J, Soerjomataram I, Siegel RL, Torre LA, Jemal A. Global cancer statistics 2018: GLOBOCAN estimates of incidence and mortality worldwide for 36 cancers in 185 countries. CA Cancer J Clin 2018; 68:394-424.
2. *Cancer registry of Norway: Cancer in Norway 2018 — Cancer incidence, mortality, survival and prevalence in Norway*. Oslo, Norway: Cancer Registry of Norway; 2019. https://www.kreftregisteret.no/globalassets/cancer-in-norway/2018/cin2018.pdf.
3. de Boer SM, Powell ME, Mileshkin L, et al. Adjuvant chemoradiotherapy versus radiotherapy alone in women with high-risk endometrial cancer (PORTEC-3): Patterns of recurrence and post-hoc survival analysis of a randomised phase 3 trial. Lancet Oncol 2019;20: 1273-1285.
4. Pecorelli S. Revised FIGO staging for carcinoma of the vulva, cervix, and endometrium. Int J Gynaecol Obstet 2009;105:103-104.
5. FIGO staging for carcinoma of the vulva, cervix, and corpus uteri. Int J Gynecol Obstet 2014;125:97-98.
6. Haldorsen IS, Salvesen HB. What is the best preoperative imaging for endometrial cancer? Curr Oncol Rep 2016;18:1-11.
7. Lin G, Lai C-H, Yen T-C. Emerging molecular imaging techniques in gynecologic oncology. PET Clin 2018;13:289-299.
8. Ytre-Hauge S, Husby JA, Magnussen IJ, et al. Preoperative tumor size at MRI predicts deep myometrial invasion, lymph node metastases, and patient outcome in endometrial carcinomas. Int J Gynecol Cancer 2015;25:459-466.
9. Fasmer KE, Gulati A, Dybvik JA, et al. Preoperative 18F-FDG PET/CT tumor markers outperform MRI-based markers for the prediction of lymph node metastases in primary endometrial cancer. Eur Radiol 2020;30:2443-2453.
10. Todo Y, Watari H, Okamoto K, et al. Tumor volume successively reflects the state of disease progression in endometrial cancer. Gynecol Oncol 2013;129:472-477.
11. Gillies RJ, Kinahan PE, Hricak H. Radiomics: Images are more than pictures, they are data. Radiology 2016;278:563-577.
12. Hatt M, Rest CCL, Tixier F, Badic B, Schick U, Visvikis D. Radiomics: Data are also images. J Nucl Med 2019;60(Suppl 2):38S-44S.
13. Rogers W, Thulasi Seetha S, Refaee TAG, et al. Radiomics: from qualitative to quantitative imaging. Br J Radiol 2020;93:20190948.
14. Schick U, Lucia F, Dissaux G, et al. MRI-derived radiomics: Methodology and clinical applications in the field of pelvic oncology. Br J Radiol 2019;92:20190105.
15. Weaver O, Leung JWT. Biomarkers and imaging of breast cancer. AJR Am J Roentgenol 2018;210:271-278.
16. Lee G, Lee HY, Park H, et al. Radiomics and its emerging role in lung cancer research, imaging biomarkers and clinical management: State of the art. Eur J Radiol 2017;86:297-307.
17. Kniep HC, Madesta F, Schneider T, et al. Radiomics of brain MRI: Utility in prediction of metastatic tumor type. Radiology 2018;290:479-487.
18. Smith CP, Czarniecki M, Mehralivand S, et al. Radiomics and radiogenomics of prostate cancer. Abdom Radiol 2019;44:2021-2029.
19. Ueno Y, Forghani B, Forghani R, et al. Endometrial carcinoma: MR imaging–based texture model for preoperative risk stratification—A preliminary analysis. Radiology 2017;284:748-757.
20. Ytre-Hauge S, Dybvik JA, Lundervold A, et al. Preoperative tumor texture analysis on MRI predicts high-risk disease and reduced survival in endometrial cancer. J Magn Reson Imaging 2018;48:1637-1647.
21. Xu X, Li H, Wang S, et al. Multiplanar MRI-based predictive model for preoperative assessment of lymph node metastasis in endometrial cancer. Front Oncol 2019;9:1007.
22. Luo Y, Mei D, Gong J, Zuo M, Guo X. Multiparametric MRI-based radiomics nomogram for predicting lymphovascular space invasion in endometrial carcinoma. J Magn Reson Imaging 2020;52:1257-1262.
23. Stanzione A, Cuocolo R, Del Grosso R, et al. Deep myometrial infiltration of endometrial cancer on MRI: A radiomics-powered machine learning pilot study. Acad Radiol 2020. https://doi.org/10.1016/j.acra.2020.02.028.
24. Soslow RA, Tornos C, Park KJ, et al. Endometrial carcinoma diagnosis: Use of FIGO grading and genomic subcategories in clinical practice: Recommendations of the International Society of Gynecological Pathologists. Int J Gynecol Pathol 2019;38(Suppl 1):S64-S74.
25. Trovik J, Wik E, Stefansson IM, et al. Stathmin overexpression identifies high-risk patients and lymph node metastasis in endometrial cancer. Clin Cancer Res 2011;17:3368-3377.
26. Nougaret S, Horta M, Sala E, et al. Endometrial cancer MRI staging: Updated guidelines of the European Society of Urogenital Radiology. Eur Radiol 2019;29:792-805.
27. Kinkel K, Forstner R, Danza FM, et al. Staging of endometrial cancer with MRI: Guidelines of the European Society of Urogenital Imaging. Eur Radiol 2009;19:1565-1574.
28. Zwanenburg A, Vallières M, Abdalah MA, et al. The image biomarker standardization initiative: Standardized quantitative radiomics for high-throughput image-based phenotyping. Radiology 2020;295:328-338.
29. Chattopadhyay S, Cross P, Nayar A, Galaal K, Naik R. Tumor size: A better independent predictor of distant failure and death than depth of myometrial invasion in International Federation of Gynecology and Obstetrics stage I endometrioid endometrial cancer. Int J Gynecol Cancer 2013;23:690-697.

30. Sozzi G, Uccella S, Berretta R, et al. Tumor size, an additional risk factor of local recurrence in low-risk endometrial cancer: A large multicentric retrospective study. Int J Gynecol Cancer 2018;28:684-691.

31. Reijnen C, IntHout J, Massuger LFAG, et al. Diagnostic accuracy of clinical biomarkers for preoperative prediction of lymph node metastasis in endometrial carcinoma: A systematic review and meta-analysis. Oncologist 2019;24:e880-e890.

32. Colombo N, Creutzberg C, Amant F, et al. ESMO-ESGO-ESTRO consensus conference on endometrial cancer: Diagnosis, treatment and follow-up. Ann Oncol 2015;117:559-581.